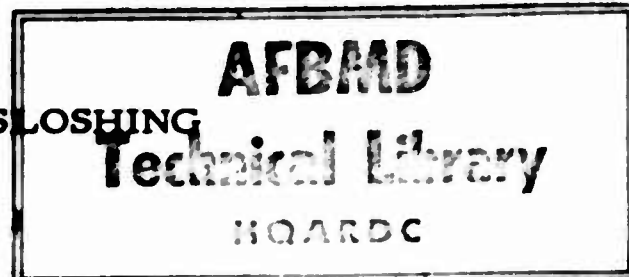


SEMIANNUAL REPORT  
ON  
EXPERIMENTAL INVESTIGATION OF SLOSHING



1 January 1959 - 30 June 1959

Prepared for the Air Force Ballistic Missile Division  
Headquarters Air Research and Development Command  
Under Contract AF 04(647)-309

Prepared by *G. P. O'Neill*  
G. P. O'Neill

Approved by *M. V. Barton*  
M. V. Barton

*G. E. Solomon*  
G. E. Solomon

SPACE TECHNOLOGY LABORATORIES, INC.  
P. O. Box 95001  
Los Angeles 45, California

AD 607341

### ABSTRACT

During the period 1 January to 30 June 1959, experimental techniques were developed for measuring slosh damping in a variety of tank and baffle configurations. The various methods were compared and shown to be in satisfactory agreement. The Able-Star damping investigation made use of one of the methods having the broadest application possibilities. A systematic variation of tank-shape parameters is continuing in support of ballistic missile programs like ATLAS, TITAN, and THOR, and in preparation for the needs of future space explorations systems.

Nonlinear damping effects were investigated. Waves sweeping across a domed tank bottom resulted in plunging flow with high but erratic damping. Waves splashing against damping rings were quickly damped, but a new slosh mode persisted with low damping. Further investigation of nonlinear effects will include measurements on the damping produced by domed roofs such as those used in the Able-Star propulsion system.

## CONTENTS

	PAGE
I. INTRODUCTION. . . . .	1
A. General. . . . .	1
B. Major Categories of the Current Investigations. . . . .	1
1. Transient Sloshing and Force Interactions. . . . .	1
2. Interaction of the Damping Ring and the Liquid Surface	2
3. Multiple-Ring Damping Effects. . . . .	2
4. Effect of Tank Configurations. . . . .	2
C. Abstract of Technical Progress. . . . .	2
D. Planned Program for the Next Period. . . . .	3
II. TECHNICAL PROGRESS. . . . .	3
A. Summary. . . . .	3
B. Ring-Damping Measurements by Programmed Transient Methods and Correlation with Steady-State Results. . . . .	4
1. Ring-Damping Theory Used as Basis for Comparison of Measurements. . . . .	4
2. Measuring Methods. . . . .	8
3. Comparison of Ring-Damping Measurements. . . . .	10
C. Interaction of the Damping Ring and the Liquid Surface. . . . .	14
1. A New Slosh Phenomenon. . . . .	14
D. Effect of Tank Configuration. . . . .	15
1. Combined Effect of Damping Rings and a Hemispherically Domed Bottom. . . . .	15
2. Damping Effect of the Hemispherically Domed Bottom. . . . .	18
E. Measuring Equipment and Techniques. . . . .	18
III. TECHNICAL PLANS. . . . .	18
A. Work Extensions. . . . .	18
1. Transient Sloshing and Nonlinear Effects. . . . .	18
2. Interaction of the Damping Ring and the Liquid Surface. . . . .	23
3. Multiple-Ring Damping Effects. . . . .	23
4. Effect of Tank Configuration. . . . .	23
B. Work Schedule	
BIBLIOGRAPHY. . . . .	25
DISTRIBUTION. . . . .	26

ILLUSTRATIONS

Figure		Page
1	Elevation Cross-Section of Cylindrical Tank with a Flat Bottom and an Annular Damping Ring. . . . .	5
2	Damping Ratios for an Annular Ring in a Cylindrical Tank with a Flat Bottom. Ring Position $(h-d)/a = 2.11$ , Ring-Width Parameter $\alpha = 0.235$ . . . . .	13
3	Elevation Cross-Section of a Cylindrical Tank with a Hemispherically Domed Bottom and an Annular Damping Ring.	16
4	Damping Ratios for an Annular Ring in a Cylindrical Tank with a Hemispherically Domed Bottom. Ring Position $(h-d)/a = 0.473$ , Ring-Width Parameter $\alpha = 0.235$ . . . . .	19
5	Damping Ratios for a Cylindrical Tank with a Hemispherically Domed Bottom. . . . .	20
6	The Slosh Test Facility with One-Degree-of-Freedom Tank Platform. . . . .	22
7	One of the Assemblies for a Variation of Tank Configuration. .	24

Tables

I	Damping Ratios for an Annular Ring in a Cylindrical Tank with a Flat Bottom. Ring Position $(h-d)/a = 2.11$ , Ring-Width Parameter $\alpha = 0.235$ . . . . .	11
II	Damping Ratios for an Annular Ring in a Cylindrical Tank with a Flat Bottom. Ring Position $(h-d)/2 = 2.11$ , Ring-Width Parameter $\alpha = 0.458$ . . . . .	12
III	Damping Ratios for an Annular Ring in a Cylindrical Tank with a Hemispherically Domed Bottom. Ring Position $(h-d)/a = 0.473$ , Ring-Width Parameter $\alpha = 0.235$ . . . . .	17
IV	Damping Ratios for a Cylindrical Tank with a Hemispherically Domed Bottom. . . . .	21

## I. INTRODUCTION

### A. General

In an earlier stage of the Experimental Investigations of Sloshing (Program Plan 165-11), data were obtained to evaluate the damping effectiveness of ring-baffle designs of the type used in the ATLAS and TITAN missiles. These data, through direct measurement of ring force, provided experimental verification of the currently used theory and resulted in an extension of the range of application of the theory. Additional measurements which were made during the current program are providing checks by independent techniques and allowing consideration of an adjustment in the empirical relationship that was used in the development of the ring-baffle theory.

Exploratory investigations were made to determine the interaction of damping rings and the liquid surface. The investigation of tank configuration was started with initial tests to determine the damping characteristics of the AJ10-104 Able-Star fuel and oxidizer tanks.

### B. Major Categories of the Current Investigation

The following four major categories of the current investigation were outlined in Project Plan 165-11 as revised for CY 1959:

#### 1. Transient Sloshing and Force Interactions

The principal objective of the current program is to develop the necessary techniques and to evaluate the slosh characteristics of tank and baffle systems by means of measurements of the response to programmed transient inputs. In carrying out this objective, it was planned to measure wave motions and forces for:

- a. Build-up (and decay) of sloshing motions as a function of frequency and time caused by a programmed input
- b. Rapid lowering of liquid level
- c. Changes in sloshing in the presence of liquid rotation.

## 2. Interaction of the Damping Ring and the Liquid Surface

The damping of a single-ring baffle breaking through the surface of the liquid was to be determined.

## 3. Multiple-Ring Damping Effects

The damping coefficients were to be determined for conditions in which two or more ring baffles are adjacent to one another as is the case in many missile applications. It was to be determined if single-ring data can be used for multiple-ring situations by the application of the principle of superposition.

## 4. Effect of Tank Configuration

In the program extension, it was indicated that various angle cones representing the bottom of missile tanks should be tested. An extended list of the configurations was not given because it was anticipated that current needs might shift the emphasis during the course of the program. Such needs, as a matter of fact, have resulted in the first measurements to determine the effects of configuration on cylindrical tanks with hemispherical end caps. The status of this series of measurements is indicated below along with the reports on other major categories of the current investigation.

### C. Abstract of Technical Progress

The majority of the activities during this report period have been directed toward the development of techniques for evaluating the slosh characteristics of tank and baffle systems through measurements of response to transients. Damping coefficients have been determined by various methods for typical configurations that are important for ballistic-missile and space-vehicle missions.

Some preliminary runs have been made to determine the interaction of the damping ring with the liquid surface. The expected very high damping was confirmed qualitatively, but the technique has not been developed to a degree of perfection allowing accurate numerical data to be obtained. During this exploration, however, accurate recordings were made of a new slosh phenomenon that had not been previously observed. The damping coefficient and frequency were measured for an example of this new mode of sloshing.

Work has not been started on the third category of investigation dealing with multiple-ring damping effects. It is believed that there is less question about how to handle such problems and that, until other effects are determined more precisely, it will be more advantageous to postpone this comparison.

The investigation of tank configuration has been started. The first runs were made with a hemispherical bottom added to the existing 1.0-foot diameter cylindrical test tank so that the hemispherical dome projected upwards into the tank. Damping coefficients were determined for various liquid levels and for the combined effects of the bottom shape and damping ring. Results are summarized below and they were used as the basis for preliminary recommendations on baffles for the AJ10-104 Able-Star fuel and oxidizer tanks.

#### D. Planned Program for the Next Period

In continuing the investigation of tank configurations, more complete variation of shape parameters will be made with new test tanks having a diameter of about 1.5 feet. There will be provision for variation in the length of the cylindrical section as well as for turning the hemispherical bottom and top caps either toward or away from the tank. The conical bottoms mentioned in the program plan can also be added to this model.

Investigations of transients and nonlinear effects will be continued. Emphasis will be placed on improving the measuring techniques for high damping rates and for a wider application to various tank and baffle configurations producing nonlinear effects.

## II. TECHNICAL PROGRESS

### A. Summary

Damping coefficient measurements have been made by five different methods on two tank and baffle configurations each at three-ring submergence ratios. At each submergence the measurements were made for a number of wave amplitudes. Three of the methods are based on measurements of the slosh response to programmed inputs. Two of the transient sloshing methods

Work has not been started on the third category of investigation dealing with multiple-ring damping effects. It is believed that there is less question about how to handle such problems and that, until other effects are determined more precisely, it will be more advantageous to postpone this comparison.

The investigation of tank configuration has been started. The first runs were made with a hemispherical bottom added to the existing 1.0-foot diameter cylindrical test tank so that the hemispherical dome projected upwards into the tank. Damping coefficients were determined for various liquid levels and for the combined effects of the bottom shape and damping ring. Results are summarized below and they were used as the basis for preliminary recommendations on baffles for the AJ10-104 Able-Star fuel and oxidizer tanks.

#### D. Planned Program for the Next Period

In continuing the investigation of tank configurations, more complete variation of shape parameters will be made with new test tanks having a diameter of about 1.5 feet. There will be provision for variation in the length of the cylindrical section as well as for turning the hemispherical bottom and top caps either toward or away from the tank. The conical bottoms mentioned in the program plan can also be added to this model.

Investigations of transients and nonlinear effects will be continued. Emphasis will be placed on improving the measuring techniques for high damping rates and for a wider application to various tank and baffle configurations producing nonlinear effects.

## II. TECHNICAL PROGRESS

### A. Summary

Damping coefficient measurements have been made by five different methods on two tank and baffle configurations each at three-ring submergence ratios. At each submergence the measurements were made for a number of wave amplitudes. Three of the methods are based on measurements of the slosh response to programmed inputs. Two of the transient sloshing methods

were also used on two additional tank and baffle configurations at various liquid levels and wave amplitudes.

Preliminary determinations were made of the interaction of the damping ring with the liquid surface. During these tests records were made of a new slosh phenomenon that had not been previously observed. Results of these measurements are given below.

#### B. Ring-Damping Measurements by Programmed Transient Methods and Correlation with Steady-State Results

During the current program, various transient methods of measurement were used to determine the damping coefficient for the cylindrical tank and single-ring baffle combinations that were previously tested by steady-state methods. The width and submergence of the ring and the water depth were held the same as used in previous tests in order that the various transient and steady-state methods could be more directly compared.

##### 1. Ring-Damping Theory Used as Basis for Comparison of Measurements

The following presentation of the results of the experimental program is based on the equations and notation used by Miles.<sup>1</sup> The cylindrical tank of radius  $a$  containing liquid to a depth  $h$  is indicated in Figure 1. An annular ring is attached to the inner wall of the tank at a distance  $d$  below the equilibrium free surface, i. e., at a distance  $h-d$  above the tank bottom. The area of the ring is  $\alpha\pi a^2$ , where  $\alpha$  is the fractional part of the cross-sectional area of the tank that is blocked by the ring. This definition of  $\alpha$  as the ring area divided by the tank area is adhered to in the experimental program - and since the ring width is not always very small as assumed in theory, the exact relation between  $\alpha$ ,  $a$ , and the ring width is used. This exact relation for the ring width is  $W_R = a(1 - \sqrt{1-\alpha})$  whereas the narrow-ring approximation is  $W_R \approx \alpha a/2$ ; or conversely, the ring width is characterized by the parameter  $\alpha$  that is determined by the exact equation

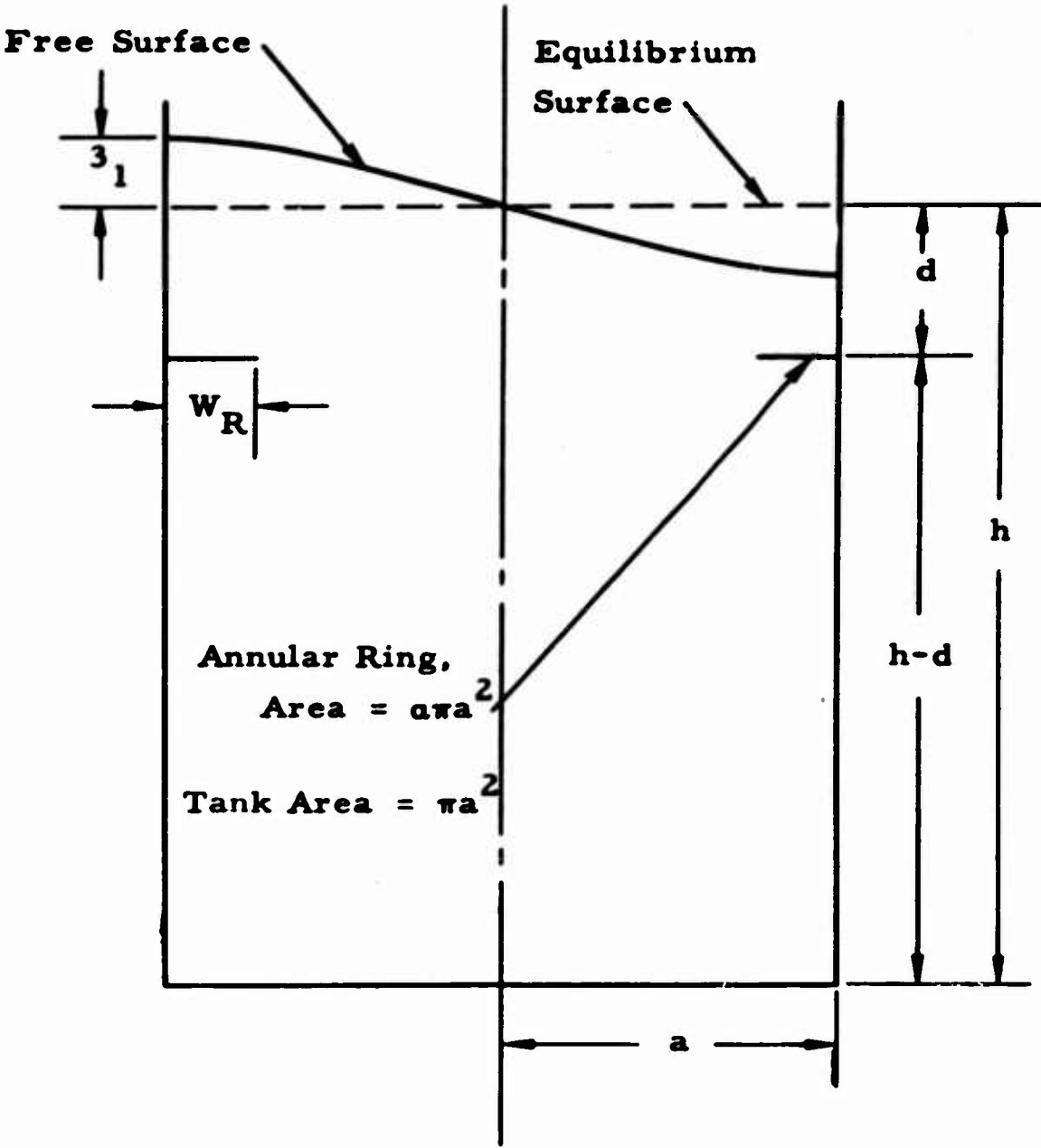


Figure 1. Elevation Cross-Section of Cylindrical Tank with a Flat Bottom and an Annular Damping Ring.

(1340)

$$\alpha = \frac{a^2 - (a - W_R)^2}{a^2} \quad (1)$$

instead of the approximation  $\alpha \approx 2 W_R/a$ .

The dominant mode of lateral slosh produces a wave amplitude that is greatest at the tank wall where the time-wise maximum is denoted by the vertical amplitude  $\xi$ . The direction of flow in the vicinity of the wall at the maximum amplitude orientation is essentially vertical and normal to any small annular ring located a small distance below the surface. Energy dissipation results from the wave motion being opposed by the ring pressure  $(\rho v^2/2)C_D$ , where  $\rho$  is the density of the fluid,  $v$  is the local wave velocity producing the pressure, and  $C_D$  is the local drag coefficient. The damping rate is determined by the amount of this dissipation per cycle as compared with the total energy of motion; or more specifically, with the logarithmic decrement  $\delta$  being  $\log_e$  of the ratio of the maximum wave amplitudes for successive slosh cycles (assuming zero input and a difference only due to the energy dissipation), the damping ratio is defined as

$$\gamma = \delta/2\pi. \quad (2)$$

By means of such energy considerations, Miles<sup>1</sup> has determined the damping ratio as

$$\gamma = \phi(ka, kd, kh) \alpha (\xi_1/a)C_D \quad (3)$$

where

$$\phi = \frac{(4/3\pi)^2 f^3(-d)ka \tanh(kh)}{1 - (1/ka)^2} \quad (4a)$$

Taking  $Ka = 1.84$  for the flat-bottomed cylindrical tank as given by Lamb<sup>2</sup> and assuming  $h > a$  so that the hyperbolic tangent may be approximated by unity and  $f(-d)$  by  $e^{-kd}$ , we obtain

$$\phi = 0.473 e^{-5.52(d/a)} \quad (4b)$$

An empirical relation for the drag coefficient was suggested by Professor Garrett Birkhoff to represent, within the limits of experimental and/or Reynolds number scatter, the measurements of Keulegan and Carpenter.<sup>3</sup> The drag coefficient was shown by their measurements to depend strongly on the path length of the cycle of oscillating flow as compared with the width of the flat plate. Characterizing this length ratio is a "period parameter"  $U_m T/D$ , where  $U_m$  denotes the time-wise maximum velocity,  $T$  the period, and  $D$  the plate width. The drag-coefficient relation suggested was

$$C_D = 15(U_m T/D)^{-1/2} \quad (5)$$

for the range  $2 \leq U_m T/D \leq 20$ .

In the present notation,

$$\frac{U_m T}{D} = \frac{[\omega \xi_1 f(-d) \cos \theta] (2\pi/\omega)}{(2\pi/a) f(-d) (\xi_1/a) \cos \theta} \quad (6)$$

where the maximum velocity term depends on the circular frequency of slosh  $\omega$ , on the wave amplitude  $\xi_1$ , on a function  $f(-d)$  of the depth of the ring, and on the position around the ring  $\theta$ ; the period term depends on the circular frequency of slosh  $\omega$ ; and the term corresponding to Keulegan and Carpenter's plate width  $D$  is twice the baffle width in consequence of the image effect at the tank wall. For flat-bottomed cylindrical tanks where  $k = 1.84$  and assuming  $h > a$ , the  $f(-d)$  term again can be replaced by  $e^{-kd}$  to give the "period parameter" in the present notation as

$$U_m T/D = (2\pi/a) e^{-1.84(d/a)} (\xi_1/a) \quad (7)$$

Using this parameter in substituting equations (5) and (4b) in Equation (3), we obtain the damping ratio

$$\begin{aligned} \gamma &= 0.473 e^{-5.52(d/a)} a (\xi_1/a)^{1.5} \left[ (2\pi/a) e^{-1.84(d/a)} (\xi_1/a) \right]^{-1/2} \\ &= 2.83 e^{-4.60(d/a)} a^{3/2} (\xi_1/a)^{1/2} \end{aligned} \quad (8)$$

as developed by Miles. This was based on the empirical relationship for the Keulegan and Carpenter data and was previously considered valid only in the range where

$$2 \leq (U_m T/D) = (2\pi/a) e^{-1.84(d/a)} (\xi_1/a) \leq 20. \quad (9)$$

The data taken during the current report period by programmed transient methods and the steady-state data previously obtained have provided experimental ring-damping determinations in the range where the theory was previously considered valid as well as for values of  $U_m T/D$  down to about 0.2.

## 2. Measuring Methods

The development of damping-measurement techniques has been stressed during this period of the program. The steady-state methods previously used were considered the most direct means of checking ring-damping theory but methods applicable to a greater variety of tank configurations were required.

In the ring-force method, a direct measurement is made of the force required to anchor the ring to the tank wall. The wave amplitude is simultaneously recorded. That component of the ring force that is out of phase with the wave velocity (i. e., opposing wave motion) results in energy dissipation; it is the amount of this dissipation as compared with the total energy of motion that determines the damping rate.

In the drive-force method, that component of the tank drive force that is in phase with the tank velocity (i. e., delivering energy to maintain steady-state oscillation) is the same as the dissipation. The damping rate for steady-state conditions is consequently determined by the amount of energy delivered to the system as compared with the energy of wave motion.

In the wave-amplitude-response method, wave amplitude as a function of drive frequency is determined for constant drive amplitude. At the dominant slosh mode, we obtain a resonant-frequency plot which is a function of the "Q" of the system or the damping ratio. Using the fundamental definition, e. g. , see Rideout.<sup>4</sup>

$$Q = 2\pi \frac{\text{Maximum stored energy}}{\text{Energy dissipated per cycle}} \quad (10)$$

the Q is shown to be equal to the ratio of the resonant frequency  $f_r$  to the half-power bandwidth  $\Delta f$ , i. e. ,

$$Q = \frac{f_r}{\Delta f} \quad (11)$$

In the assumed linear system, the half-power points for maximum stored energy are the 70.7 per cent points on the wave amplitude response curves. By measuring the band width  $\Delta f$  and the mid-frequency or resonant frequency  $f_r$  from these 0.707-of-maximum amplitude points and through use of the relation, e. g. , see Terman.<sup>5</sup>

$$\delta = \frac{\pi}{Q} \quad (12)$$

that follows from the definitions of Q and the logarithmic decrement  $\delta$ , Equations (2), (11), and (12) give the damping ratio as

$$\gamma = \frac{1}{2Q} \quad (13)$$

and

$$\gamma = \frac{\Delta f}{2f_r} \quad (14)$$

Damping ratios were determined by this method as an approximation since strict application would require that the damping be viscous rather than vary

as  $(\xi_1/a)^{1/2}$ . Since the information that is taken from the records is for peak and 70.7 per cent peak amplitude, the wave amplitude associated with the damping coefficient was taken as 85 per cent of peak.

The wave-amplitude-decay method makes use of measured wave amplitude decay after cessation of tank drive. With zero input, the decreasing energy of motion as evidenced by decreasing wave height is due to the energy dissipation by the damping mechanism. The logarithmic decrement is  $\log_e$  of the ratio of successive wave heights. The damping ratio is then given by this logarithmic decrement divided by  $2\pi$  as indicated in Equation (2).

Observation of the response to a transient, i. e. , cessation of tank drive, is also used in the anchor-force-decay method. In the assumed linear system, the peak force in the rigid anchor is proportional to the peak wave amplitude as used in the above method. The logarithmic decrement is then  $\log_e$  of the ratio of successive anchor-force peaks. The damping ratio is determined again by Equation (2). This method has the widest application since no direct observation of the internal sloshing mechanism is required. The effect of the sloshing in terms of lateral force is measured; and it is this effect that is generally most pertinent to missile stability.

### 3. Comparison of Ring-Damping Measurements

The measured damping ratios as a function of wave amplitude are summarized in Tables I and II. Data are given for the above five measuring methods applied to two ring widths each at three values of submergence.

In developing the ring-damping theory, the assumption was made that the ring is small enough and submerged deep enough that the gross flow pattern of the slosh wave is not affected. The data for conditions conforming most closely to these assumptions are plotted in Figure 2. At the deeper of the two plotted values of submergence where  $(d/a) = 0.505$ , measurements by the two decay methods agree with the theory given in Equation (8). The ring-force and the drive-force methods gave values that are lower than the theory predicts while the approximations by the wave-amplitude-response method are higher than theory. Recognizing the approximations and the difficulties of

Table 1. Damping Ratios for an Annular Ring in a Cylindrical Tank with a Flat Bottom. Ring Position  $(h-d)/a = 2.11$ , Ring-width Parameter  $\alpha = 0.235$ .

Method of Damping Measurement	$\frac{d}{a} = 0.168$		$\frac{d}{a} = 0.253$		$\frac{d}{a} = 0.505$	
	$\xi_1/a$	$\gamma$	$\xi_1/a$	$\gamma$	$\xi_1/a$	$\gamma$
Ring Force	0.050	0.019	0.15	0.026	0.19	0.0085
	0.082	0.024	0.12	0.027	0.17	0.0071
	0.11	0.027	0.11	0.026	0.16	0.0075
	0.090	0.023			0.14	0.0064
	0.064	0.024			0.13	0.0061
Drive Force	0.050	0.029	0.15	0.027	0.19	0.012
	0.082	0.025	0.12	0.031	0.17	0.0093
	0.11	0.026	0.11	0.031	0.16	0.0091
	0.090	0.021			0.14	0.0094
	0.064	0.027			0.13	0.0079
Wave Amplitude Response	0.28	0.18	0.23	0.040	0.21	0.023
	0.28	0.18	0.23	0.042	0.21	0.024
Wave Amplitude Decay	0.044	0.020	0.052	0.016	0.032	0.0055
	0.029	0.015	0.040	0.014	0.023	0.0052
	0.042	0.026	0.031	0.013	0.017	0.0052
	0.024	0.019	0.022	0.010	0.013	0.0044
	0.015	0.014	0.017	0.0090	0.034	0.0065
	0.036	0.030	0.051	0.012	0.028	0.0047
	0.027	0.030	0.039	0.012	0.024	0.0044
	0.017	0.021	0.026	0.015	0.021	0.0047
	0.012	0.019	0.020	0.011		
	0.0085	0.017	0.015	0.0087		
0.0060	0.015					
Anchor Force Decay	0.042	0.017	0.052	0.025	0.032	0.0079
	0.024	0.017	0.040	0.016	0.023	0.0059
	0.015	0.012	0.031	0.014	0.017	0.0047
	0.036	0.026	0.022	0.011	0.013	0.0039
	0.027	0.020	0.051	0.022	0.034	0.0062
	0.017	0.022	0.039	0.015	0.028	0.0052
	0.012	0.015	0.026	0.011	0.024	0.0058
	0.0085	0.014	0.020	0.010	0.021	0.0041
	0.0060	0.014	0.015	0.010		

Table 2. Damping Ratios for an Annular Ring in a Cylindrical Tank with a Flat Bottom. Ring Position ( $h-d/a = 2.11$ , Ring-Width Parameter  $a = 0.458$ ).

Method of Damping Measurement	$\frac{d}{a} = 0.168$		$\frac{d}{a} = 0.253$		$\frac{d}{a} = 0.505$	
	$\xi_1/a$	$\gamma$	$\xi_1/a$	$\gamma$	$\xi_1/a$	$\gamma$
Ring Force	0.044	0.076	0.096	0.056	0.11	0.014
	0.049	0.086	0.087	0.055	0.18	0.020
	0.044	0.081	0.070	0.036	0.18	0.019
	0.031	0.0029	0.089	0.086	0.16	0.017
	0.038	0.072	0.053	0.032	0.19	0.021
	0.047	0.045	0.059	0.055	0.17	0.0086
	0.037	0.021	0.092	0.064	0.19	0.016
			0.094	0.064	0.13	0.018
			0.048	0.029	0.20	0.020
			0.066	0.039	0.16	0.018
			0.056	0.049	0.15	0.024
			0.030	0.046	0.17	0.0099
			0.030	0.041	0.15	
Drive Force			0.096	0.059	0.11	0.014
			0.070	0.057	0.18	0.017
			0.089	0.067	0.18	0.015
			0.053	0.18	0.19	0.019
			0.059	0.086	0.17	0.022
			0.092	0.077	0.19	0.019
			0.094	0.077	0.13	0.016
			0.049	0.014	0.20	0.016
			0.066	0.078	0.16	0.027
			0.056	0.11	0.15	0.020
		0.030	0.014	0.17	0.052	
				0.15	0.017	
Wave Amplitude Response	0.27	0.052	0.35	0.024	0.27	0.0078
	0.33	0.048	0.32	0.035	0.26	0.015
	0.26	0.044	0.36	0.028	0.28	0.012
	0.26	0.052	0.22	0.038	0.26	0.018
	0.33	0.046				
	0.26	0.044				
Wave Amplitude Decay	0.025	0.085	0.032	0.038	0.037	0.015
	0.017	0.061	0.026	0.038	0.026	0.014
	0.012	0.055	0.016	0.033	0.017	0.011
	0.0085	0.055	0.011	0.026	0.012	0.0091
	0.006	0.050	0.0085	0.023		
		0.0065	0.016			
	0.025	0.081	0.026	0.039	0.036	0.019
	0.017	0.058	0.016	0.042	0.026	0.015
	0.012	0.036	0.011	0.015	0.017	0.0094
	0.0085	0.041	0.0085	0.024	0.012	0.0085
	0.006	0.011	0.0065	0.017		

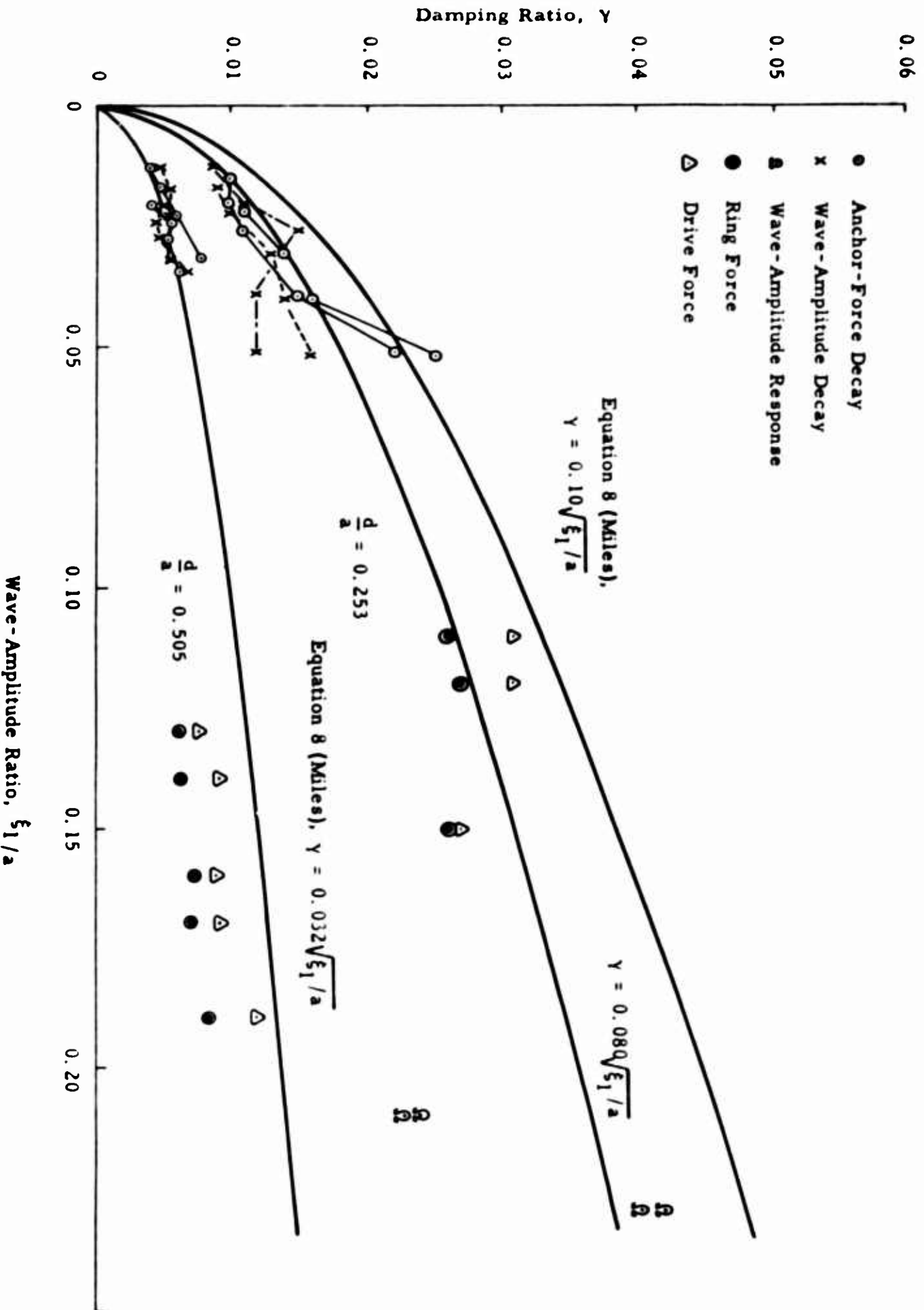


Figure 2. Damping Ratios for an Annular Ring in a Cylindrical Tank with a Flat Bottom. Ring Position  $(h-a)/a = 2.11$ , Ring-width Parameter  $\alpha = 0.235$ .

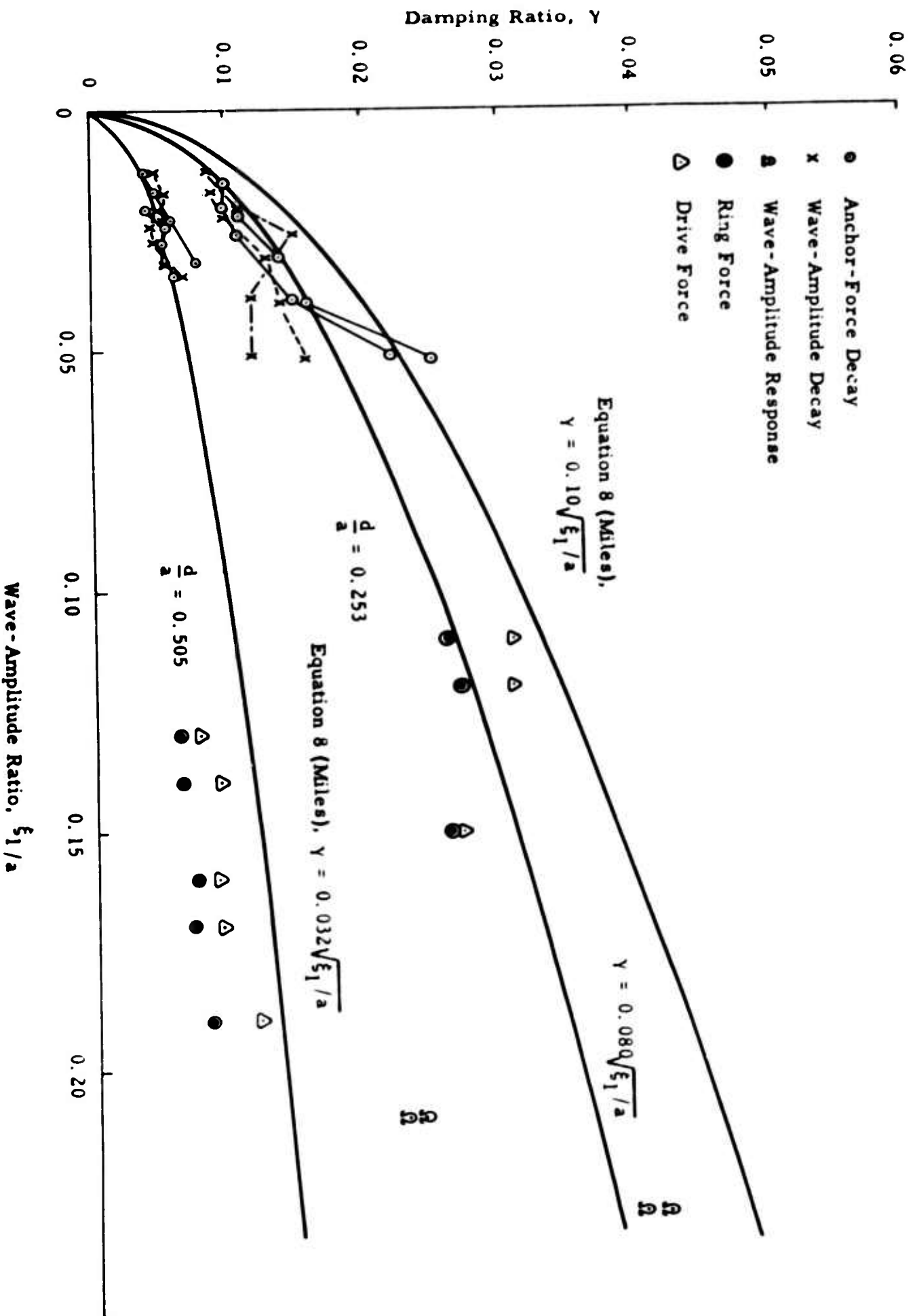


Figure 2. Damping Ratios for an Annular Ring in a Cylindrical Tank with a Flat Bottom. Ring Position  $(h-d)/a = 2.11$ , Ring-width Parameter  $\alpha = 0.235$ .

(1241)

measuring the low components of ring force opposing the wave velocity and the low components of drive force in phase with the tank velocity, this data is considered in agreement with theory.

For the shallower of the two values of submergence where  $(d/a) = 0.253$ , the data agree with the prediction of  $\gamma \approx (\xi_1/a)^{1/2}$  but the values are about 20 per cent lower than the results given by Equation (8). This should possibly be considered as reasonable agreement, however, the deviation indicated at one ring depth and the absence of a confirmed deviation at the other does lead one to question whether the measured damping is following the exponential depth relation.

### C. Interaction of the Damping Ring and the Liquid Surface

The expected very high damping was qualitatively confirmed for the case where the damping ring breaks through the free surface during a slosh cycle. Since the technique has not been developed to a degree of perfection allowing accurate numerical data to be obtained, it is recommended that the submerged-ring theory be used.

#### 1. A New Slosh Phenomenon

During the course of the ring-splashing explorations, accurate recordings were made of a new slosh phenomenon which had not been previously observed. When the damping ring was mounted at the free surface, large waves that splashed against the ring at the normal first-mode frequency were highly damped. An oscillation of small amplitude persisted, however, with very low damping. Its frequency was higher than the normal first-mode frequency but not as high as the second-mode frequency.

The circular frequency for lateral sloshing oscillations having one nodal diameter at the surface of a liquid in a cylindrical tank is given by

$$\omega^2 = kg \tanh(kh) \quad (15)$$

where  $g$  is the uniform local acceleration that is directed along the axis of the tank, and the slosh modes in a flat-bottomed tank are governed by the relations. <sup>2</sup>

$$ka = 1.84, 5.33, 8.54 \quad (15a)$$

Agreement between the calculated and measured frequencies was reported in the previous semiannual report. <sup>6</sup> The slosh frequency at the beginning of the record of ring-splash damping was very close to the calculated frequency ( $f = \omega/2\pi$ ) of 1.74 cps for the first mode ( $a = 0.495$  ft,  $h = 1.04$  ft). After a few cycles at high damping, the wave no longer splashed against the ring; the anchor-force-decay record, however, showed a shift to a new frequency of 2.04 cps for a small wave that persisted and was principally confined to the region inside the ring. This new slosh mode had the very low damping ratio of  $\gamma = 0.0023$ .

The new slosh mode which is caused by the presence of the ring has a resonant frequency between the first tank mode frequency (1.74 cps) and the second (2.97 cps). It is therefore a new lateral slosh mode which is not present in the tank without baffles. Interference with missile stability is not to be expected, however, because the wave could not be large in amplitude without causing flow around the baffle with consequent restoration of the higher damping.

#### D. Effect of Tank Configuration

The first part of the program on the investigation of various tank configurations was directed towards determining the damping requirements for the Able-Star fuel and oxidizer tanks. Preliminary tests had been made at the end of the current report period and were used as the basis for preliminary baffle recommendations.

##### 1. Combined Effect of Damping Rings and a Hemispherically Domed Bottom

A hemispherically domed bottom was added to the existing 1.0 ft. diameter cylindrical test tank. The defining cross-section for the position of the damping ring and dome is shown in Figure 3. The measured damping ratios as a function of wave amplitudes are summarized in Table 3. The measurements

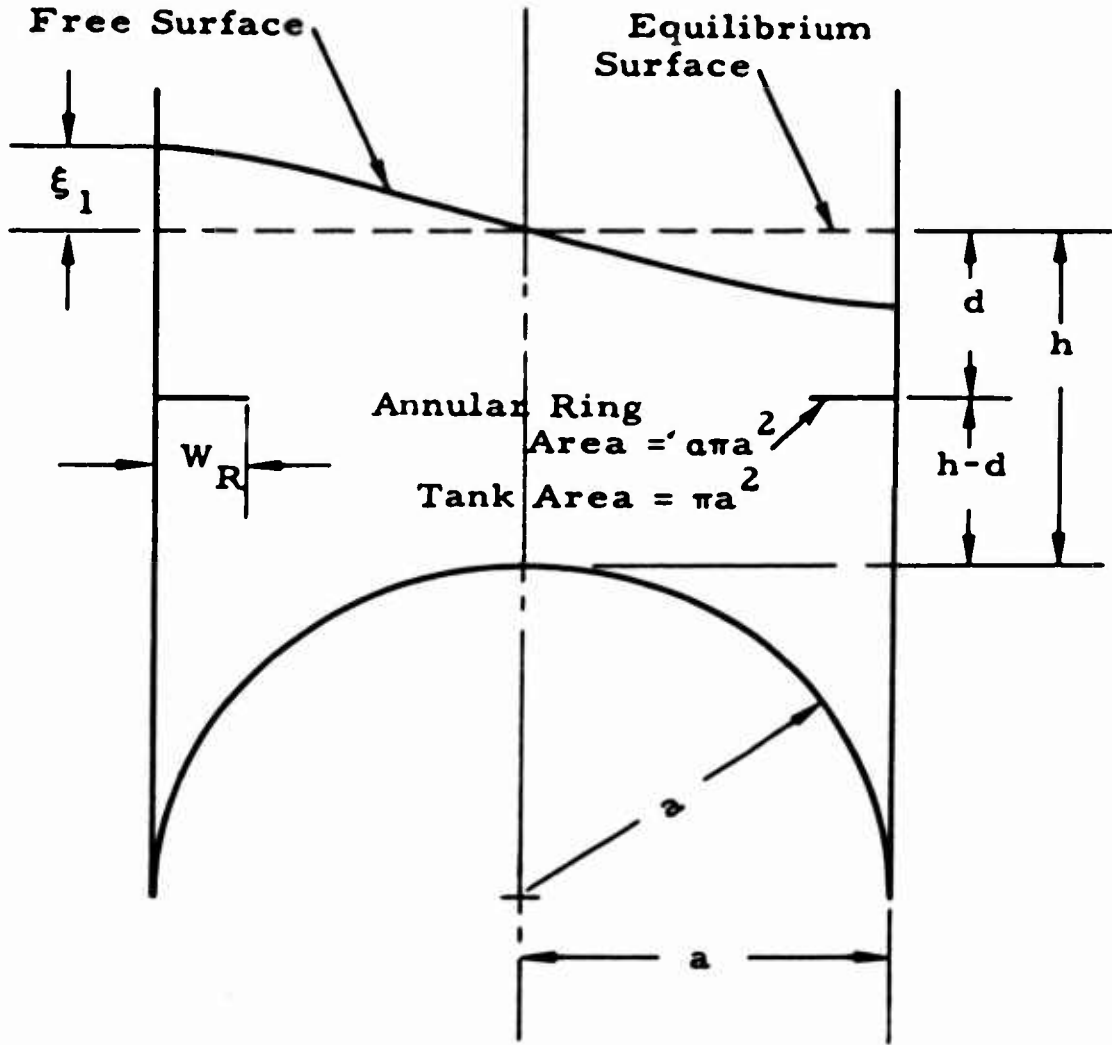


Figure 3. Elevation Cross-Section of a Cylindrical Tank with a Hemispherically Domed Bottom and an Annular Damping Ring.

(1339)

**Table 3. Damping Ratios for an Annular Ring in a Cylindrical Tank with a Hemispherically Domed Bottom. Ring Position  $(h-d)/a = 0.473$ , Ring-Width Parameter  $a = 0.235$ .**

Method of Damping Measurement	$\frac{d}{a} = 0.168$		$\frac{d}{a} = 0.379$	
	$\xi_1/a$	$\gamma$	$\xi_1/a$	$\gamma$
Wave Amplitude Decay	0.20	0.043	0.24	0.020
	0.12	0.036	0.16	0.019
	0.10	0.040	0.11	0.018
	0.08	0.032	0.08	0.013
	0.05	0.029	0.12	0.017
	0.16	0.043	0.08	0.013
	0.12	0.040	0.06	0.010
	0.09	0.032	0.05	0.010
	0.06	0.027	0.03	0.0085
	0.04	0.028	0.02	0.0074
	0.10	0.035	0.02	0.0061
	0.06	0.030	0.02	
	0.03	0.022		
	0.02	0.018		
	0.04	0.038		
	0.03	0.026		
	0.02	0.021		
0.02	0.016			
0.01	0.012			
Anchor Force Decay	0.20	0.036	0.24	0.015
	0.13	0.037	0.16	0.016
	0.098	0.032	0.11	0.013
	0.076	0.030	0.08	0.013
	0.053	0.021	0.12	0.015
	0.16	0.038	0.08	0.013
	0.12	0.036	0.06	0.0096
	0.09	0.026	0.05	0.011
	0.06	0.018	0.03	0.0082
	0.04	0.023	0.02	0.0078
	0.10	0.041	0.02	0.0061
	0.06	0.026		
	0.03	0.027		
	0.02	0.016		
	0.04	0.035		
	0.03	0.028		
	0.02	0.017		
0.02	0.015			
0.01	0.012			

were made by both the anchor-force and the wave-amplitude-decay methods. The results are plotted in Figure 4 where it is shown that the square-root relation between wave amplitude and damping ratio fits the data. This might be expected since, for the water elevations tested, the damping is principally from the ring.

## 2. Damping Effect of the Hemispherically Domed Bottom.

With the ring removed, the defining sketch of Figure 3 is used but only the water level  $h$  relative to the top of the dome is pertinent. Preliminary data is given in Table 4 and plotted in Figure 5. It is noted that for a level only one quarter radius above the dome, the waves are smooth and the damping is low and possibly viscous since there is no variation with wave amplitude. When the water is level with the dome, the damping is high and erratic since flow across the top of the dome plunges and dissipates more energy. This is a very nonlinear effect with the consequent multivalued possibilities.

## E. Measuring Equipment and Techniques.

The slosh-test facility is shown in Figure 6. An improved method of varying the slosh-drive frequency has been provided in order to facilitate resonance-curve plotting. The drive-force dynamometer becomes the anchor-force pickup device after cessation of the drive. Very little additional equipment was necessary in order to check the new techniques for measuring damping. Records were made on general-purpose laboratory recorders and X-Y plotters.

# III. TECHNICAL PLANS

## A. Work Extensions

Investigations of transient sloshing and nonlinear effects and measurements of the damping for various tank configurations are planned in order to support ballistic-missile developments and space-vehicle missions.

### 1. Transient Sloshing and Nonlinear Effects.

Observations of the decay of slosh motions have been the most valuable means of determine damping. Study of the buildup of slosh motions

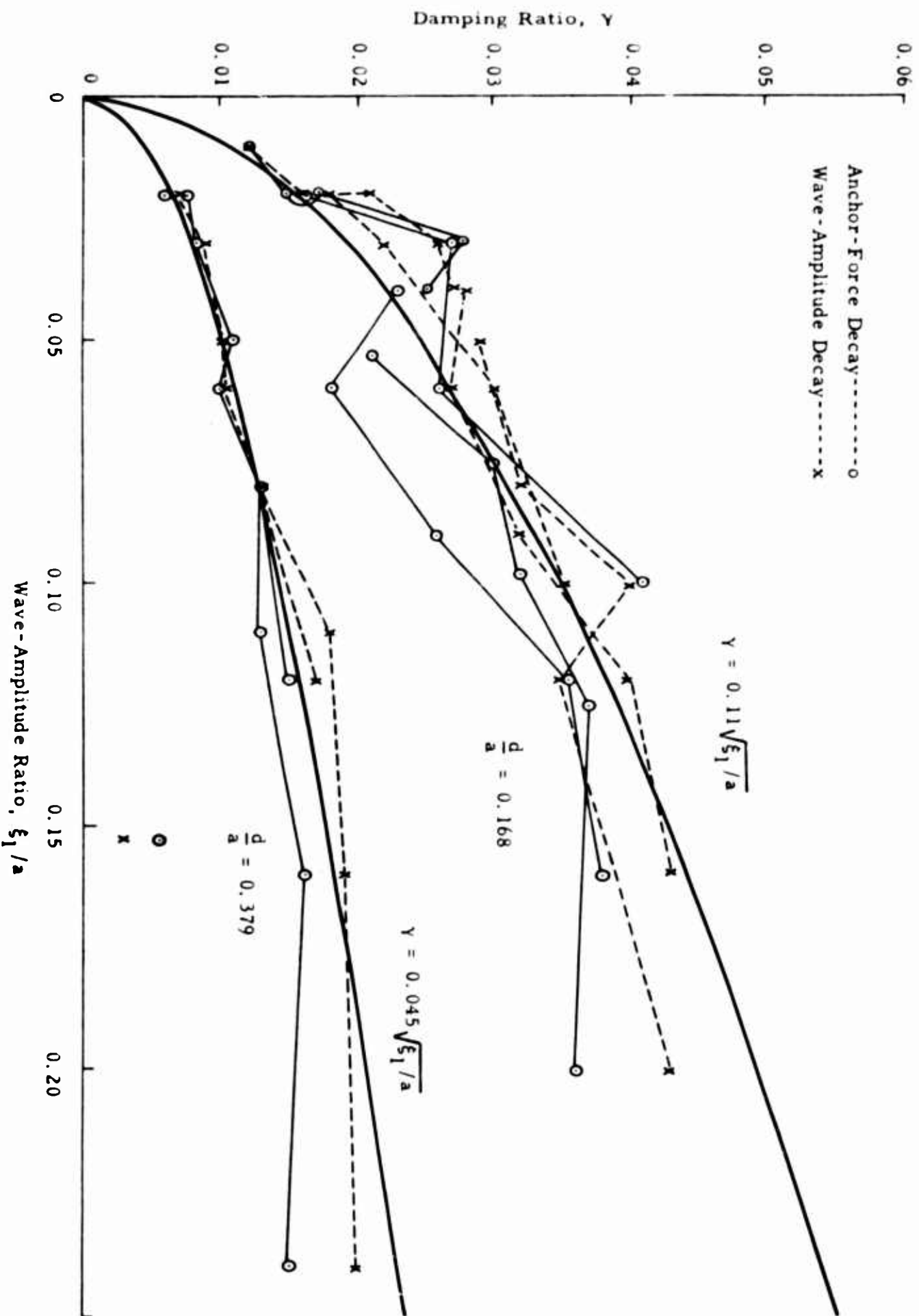


Figure 4. Damping Ratios for an Annular Ring in a Cylindrical Tank with a Hemispherically Domed Bottom. Ring Position  $(h-d)/a = 0.473$ , Ring-width Parameter  $\alpha = 0.235$ .

(1240)

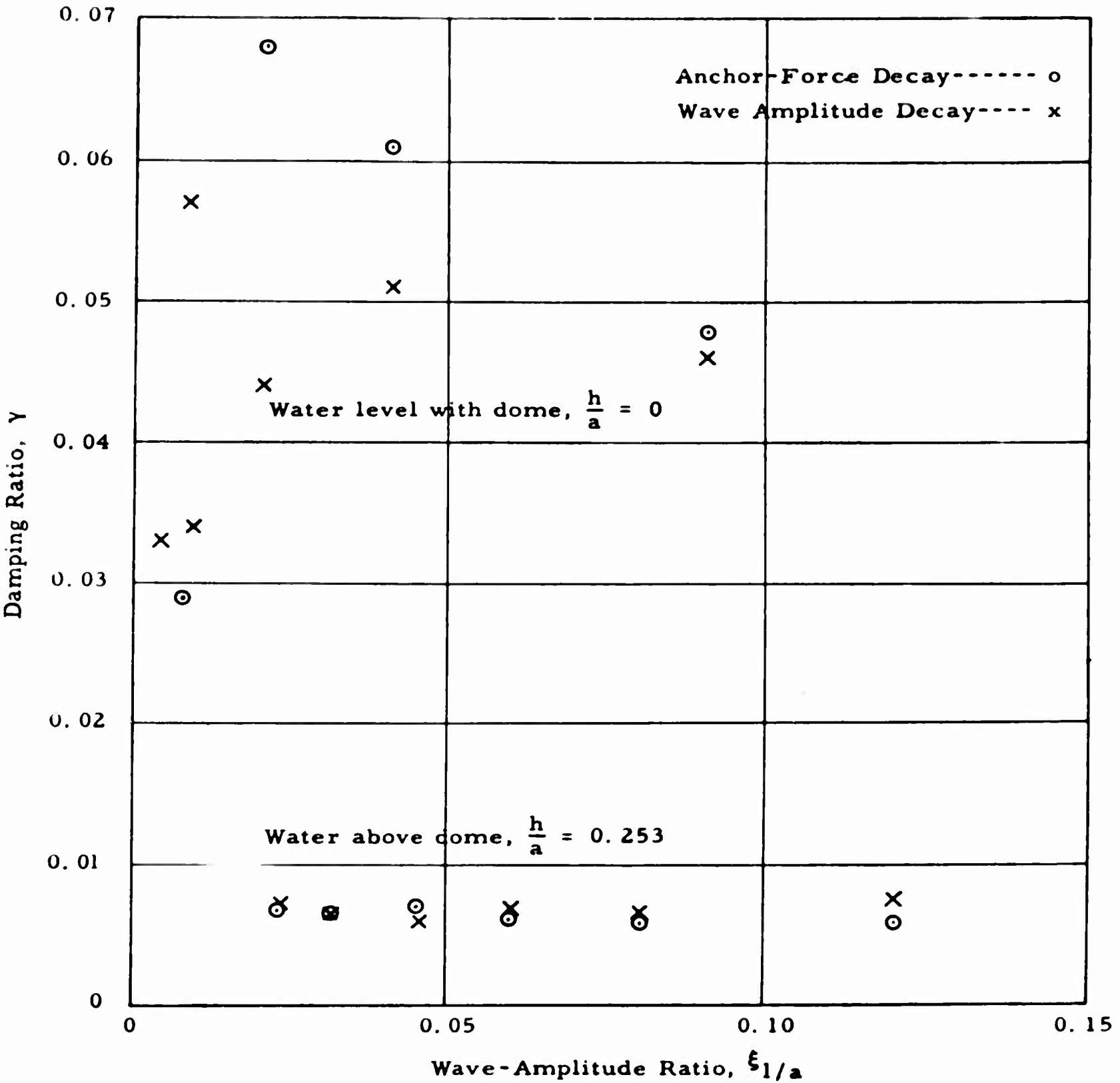
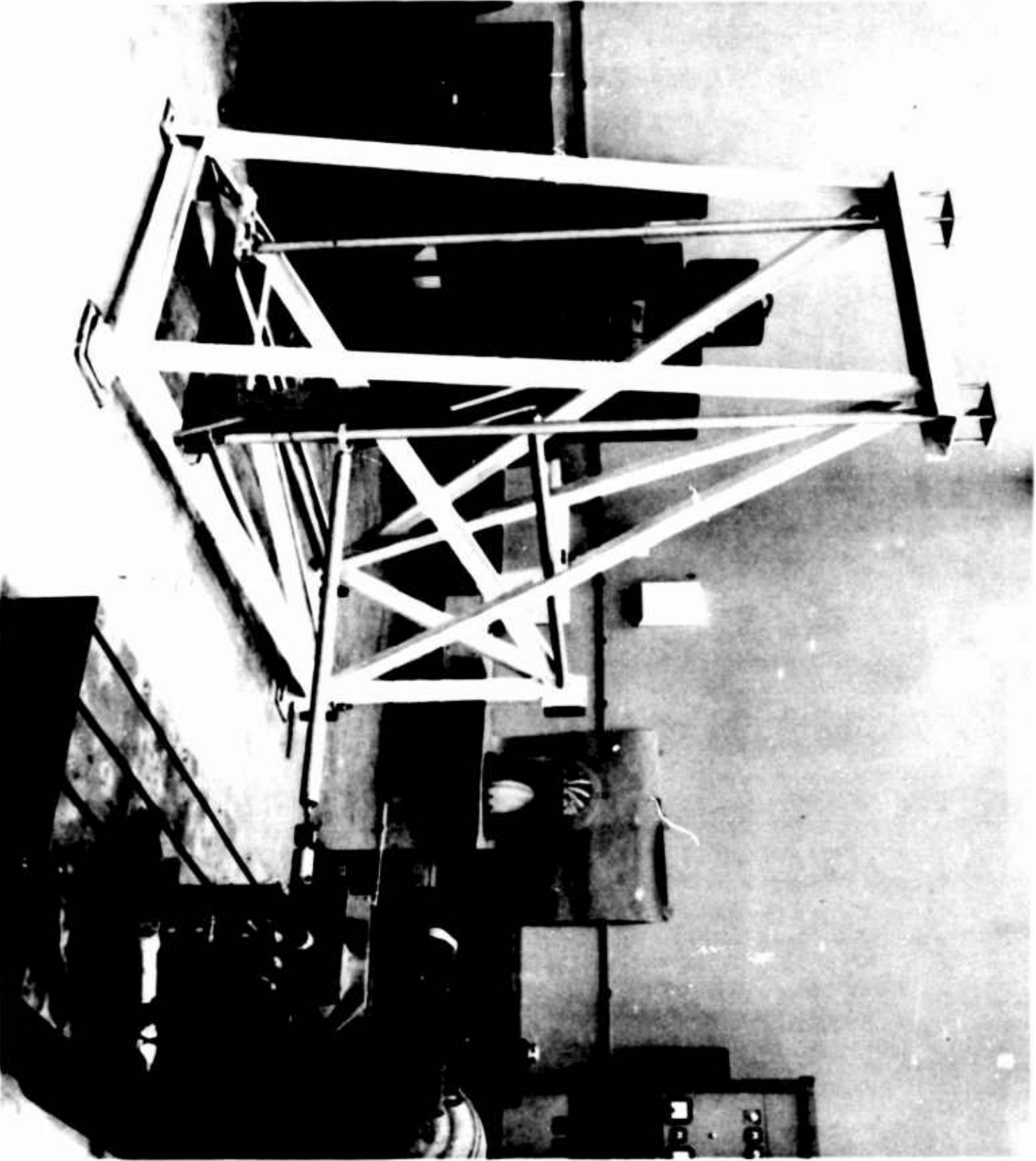


Figure 5. Damping Ratios for a Cylindrical Tank with a Hemispherically Domed Bottom.

Table 4. Damping Ratios for a Cylindrical Tank with a Hemispherically Domed Bottom.

Method of Damping Measurement	Water Level with Dome: $\frac{h}{a} = 0$		Water Above Dome: $\frac{h}{a} = 0.253$	
	$\xi_1/a$	$\gamma$	$\xi_1/a$	$\gamma$
Wave Amplitude Decay	0.02	0.044	0.045	0.0059
	0.009	0.034	0.032	0.0065
	0.004	0.033	0.023	0.0072
	0.09	0.046	0.12	0.0073
	0.04	0.051	0.08	0.0064
	0.008	0.057	0.06	0.0069
Anchor Force Decay	0.02	0.068	0.045	0.0070
	0.008	0.029	0.032	0.0065
	0.09	0.048	0.023	0.0067
	0.04	0.061	0.12	0.0059
			0.08	0.0059
		0.06	0.0061	

Figure 6. The Slosh Test Facility with One-Degree-of-Freedom Tank Platform.



in response to a programmed input will also be investigated as a possible method that is more analogous to the situation encountered in a vehicle mission.

2. Interaction of the Damping Ring and the Liquid Surface.

As methods for measuring high damping and nonlinear effects are developed or improved, they will be applied to the ring-splashing problem.

3. Multiple-Ring Damping Effects.

Unless current propulsion systems require baffles so close together that the lower baffle is in the eddy produced by the upper, current methods of combining baffle damping, or the conservative practice of ignoring the lower baffle, could not be improved upon. It is not expected that the accuracy of measurement will be improved sufficiently to warrant pursuing this problem.

4. Effect of Tank Configuration.

Tank configurations of interest for current vehicle missions will be tested. This includes the Able-Star tanks for which tests are in progress. A 1.5 ft diameter scale model of one of these tanks is shown in Figure 7. This specific configuration will be followed by a breakdown of the tank configuration parameters to determine separately the damping effects of the hemispherically domed bottom and roof.

B. Work Schedule.

The work schedule is dictated by current needs in vehicle development programs. The first part of the next period will be devoted to damping determinations for Able-Star tanks and the associated basic configurations. This will be followed by the investigations of transient sloshing and nonlinear effects. Improvements and extensions of the measuring techniques will be made in order to provide experimental support to analytical and design work for future ballistic-missile and space-exploration programs.

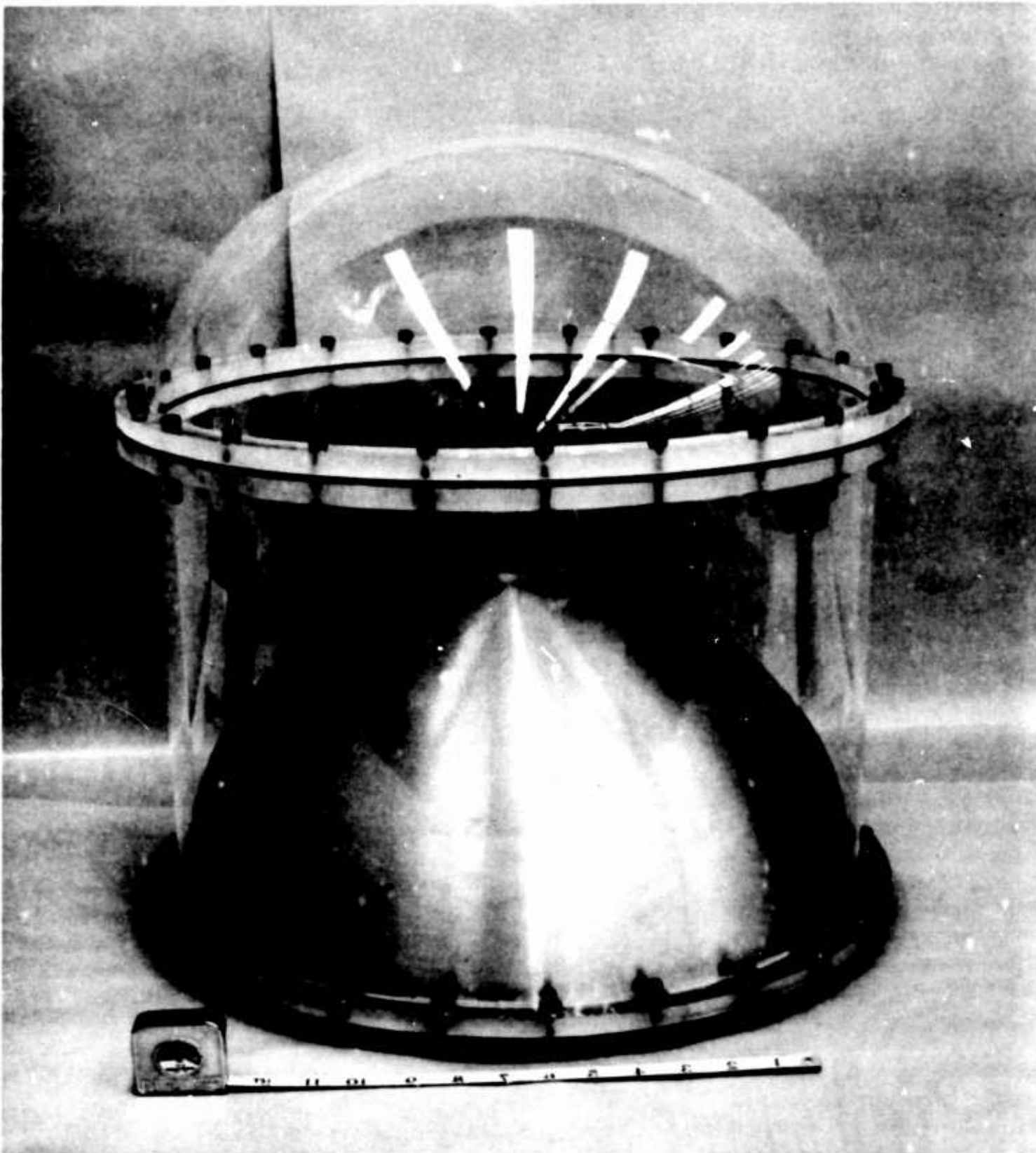


Figure 7. One of the Assemblies for a Variation of Tank Configuration.

(1240)

### BIBLIOGRAPHY

1. Miles, J. W., "Ring Damping of Free Surface Oscillations in a Circular Tank," ASME Applied Mechanics Division, Paper No. 57-A-31, 18 March 1957.
2. Lamb, H., Hydrodynamics, Dover Publications, sixth edition, (New York, 1945) p 285.
3. Keulegan, G. H. and L. H. Carpenter, "Forces on Cylinders and Plates in an Oscillating Fluid," National Bureau of Standards Report 4821, Washington, D. C., 5 September 1956.
4. Rideout, Vincent C., "Active Networks," Prentice-Hall Electrical Engineering Series, Prentice-Hall, Inc. (New York, 1954) pp 143-4.
5. Terman, Frederick Emmons, Radio Engineer's Handbook, McGraw-Hill Book Co., Inc., (New York, 1943) p 139.
6. "Semiannual Report on Experimental Investigation of Sloshing," 1 July 1958 to 31 December 1958, GM-TR-0165-00582, Space Technology Laboratories, Inc.

## DISTRIBUTION

## WDSOT

E. Atler	G. J. Gleghorn
M. V. Barton	F. W. Hesse
J. G. Berry	H. W. Johnson
E. P. Blackburn	A. Kaplan
J. Bricca	J. W. Miles
R. Bromberg	G. E. Mueller
R. M. Cooper	J. P. O'Neill (2)
R. D. De Lauer	N. Ott
R. B. Dreizler	D. N. Pitts
W. Duke	A. Rasumoff
L. G. Dunn	O. Rouse
A. T. Ellis	G. E. Solomon
D. P. Fitzgibbon	F. C. Thurston (2)
D. L. Forbes (22 + 1 reproducible)	M. W. Trembath

STL Library (2)